We are IntechOpen, the world's leading publisher of Open Access books
Built by scientists, for scientists

6,900
Open access books available

185,000
International authors and editors

200M
Downloads

Our authors are among the

154
Countries delivered to

TOP 1%
most cited scientists

12.2%
Contributors from top 500 universities

WEB OF SCIENCE™

Selection of our books indexed in the Book Citation Index in Web of Science™ Core Collection (BKCI)

Interested in publishing with us?
Contact book.department@intechopen.com

Numbers displayed above are based on latest data collected.
For more information visit www.intechopen.com

20

Advances in Interfacial Adsorption Thermodynamics: Metastable-Equilibrium Adsorption (MEA) Theory

Gang Pan, Guangzhi He and Meiyi Zhang
State Key Laboratory of Environmental Aquatic Chemistry, Research Center for Eco-Environmental Sciences, Chinese Academy of Sciences, People's Republic of China

1. Introduction

Interfacial processes are central to understanding many processes in environmental sciences and technologies, chemical engineering, earth sciences, ocean sciences and atmospheric sciences. Thermodynamics has been used as a classical method to describe interfacial equilibrium properties over the last century. Experimentally measurable macroscopic parameters of adsorption density and concentration are widely used as the basic parameters in many equations/models to describe the equilibrium characteristics of adsorption reactions at solid-water interfaces. For instance, methods of equilibrium adsorption constants or adsorption isotherms are commonly used to describe the equilibrium relationship between concentration in solution and adsorption density on solid surfaces.

However, thermodynamics has limitations in describing the equilibrium properties for surface adsorption reactions at solid-water interfaces. A fundamental principle has been missing in the conventional theoretical system where the microscopic structures on the solid surfaces are not taken into account in the conventional macroscopic methodology such as equilibrium adsorption constants and/or adsorption isotherms. The equilibrium properties for surface adsorption were conventionally described by macroscopic parameters such as adsorption density. Unfortunately, adsorption density is not a thermodynamic state variable and is generally affected by the microscopic metastable equilibrium surface structures, which make the equilibrium properties, such as equilibrium constants and/or adsorption isotherms, be fundamentally dependent on the kinetic paths and/or the reactant concentration conditions (e.g. the "adsorbent concentration effect" and "adsorbate concentration effect"). Failure in recognizing this theoretical gap has greatly hindered our understanding on many adsorption related issues especially in applied science and technology fields where the use of surface concentration (mol/m^2) is common and inevitable.

With the application of spectroscopy and quantum chemical calculation techniques to solid-liquid interface systems, such as synchrotron based X-ray absorption spectroscopy, it is now possible to develop new thermodynamic methodologies to describe the real equilibrium properties of surface adsorption reactions and to reveal the relationships between macroscopic equilibrium properties and the microscopic metastable equilibrium adsorption

(MEA) structures. These studies represent advances on how microscopic surface molecule structures affect the macroscopic relationships in surface adsorption thermodynamics. Surface microstructures greatly affect the local chemical properties, long-range interaction, surface reactivity, and bioavailability of pollutants in the environment. Both experimental techniques and thermodynamic theoretical development on interfacial processes are essential for the development of molecular environmental and geological sciences.

It has been a basic concept in traditional thermodynamic adsorption theories that adsorption density (Γ , mol/m^2) is a state variable (a function that is only determined by the state and not affected by the path), so that the equilibrium adsorption constants defined by the ratio of equilibrium adsorption density on solid surfaces to the concentration in solution should be constant that is the reflection of the unique equilibrium characteristic of the reaction.[1] Over the last century, the macroscopic methodology (e.g. surface complexation models) of equilibrium adsorption constants and adsorption isotherms are widely used to describe the equilibrium limits of adsorption reactions and predict the theoretical yield in many fields.[2, 3] These relationships were deemed to obey the basic properties of chemical thermodynamics, i.e. the equilibrium constant should be constant and be independent of kinetics or initial reactant concentrations under fixed thermodynamic conditions.

However, an abnormal phenomenon called particle/adsorbent concentration effect (C_p effect), i.e. the dependence of adsorption isotherms on one of the reactant concentrations C_p, has caused great confusion over the last three decades because it cannot be interpreted by the existing thermodynamic theories.[2, 4-8] Several hundreds of papers have been published on this issue but the underlined theoretical reason, which is far more important than the C_p effect itself, still remains not clear to most researchers. Most studies so far attribute C_p effect to various experimental artifacts.[9, 10] However, after these artifacts are excluded from the experiments, C_p effect may disappear in some systems,[9] but still exist in other systems.[3, 11] Thus, the problem becomes rather confused based on empirical or experimental analysis only.

Metastable-equilibrium adsorption (MEA) theory indicates that,[12-14] for a given adsorption reaction under fixed thermodynamic conditions, a polyhedral adsorbate molecule is generally ended in various MEA states with different energies and geometries rather than a unique equilibrium state when the reaction reaches to the apparent equilibrium. Unlike concentration in solutions, adsorption density (mol/m2) on solid surfaces no longer unambiguously corresponds to thermodynamic state variables, because adsorption density can only count for the mass but not the chemical potentials/energies of different microscopic MEA states that construct the real equilibrium adsorption state. When the adsorption density is not treated as a thermodynamic state variable, a theoretical equation known as "MEA inequality" is deducted from the fundamental thermodynamic laws.[12]

2. Metastable-equilibrium adsorption inequality

Suppose the adsorption of a pure solute A in a pure solvent onto a solid surface can be schematically represented by the equation (1, 2)

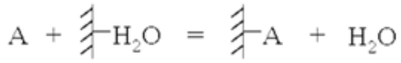

(1)

where A stands for solute in solution, $\equiv H_2O$ for adsorbed solvent, $\equiv A$ for adsorbed A, and H_2O for solvent in solution.

Since the Gibbs free energy is a state function and its change depends only on the initial and final states of the system, we can replace the real adsorption process of [1], which is generally thermodynamically irreversible, with two ideal reversible processes that lead to the same final state, in order to calculate the Gibbs free energy change,

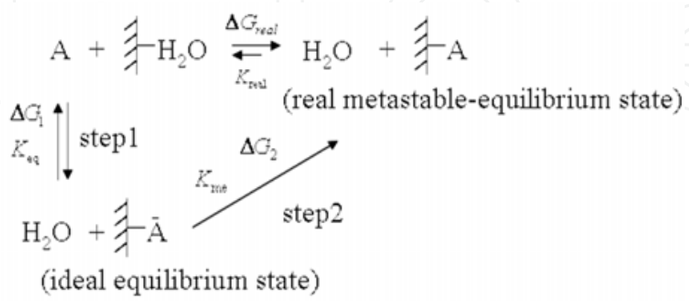

(2)

where "$\rightleftharpoons$" indicates that the real adsorption process can be irreversible. Step 1 represents an imagined reversible adsorption process where the final concentration of *A* on the solid surface is the same as that in the real irreversible process [1]. $\equiv \bar{A}$ represents an ideal equilibrium stable state of adsorbed *A*, and $\equiv A$ represents a real metastable-equilibrium adsorption state. $\equiv \bar{A}$ and $\equiv A$ represent different thermodynamic states of adsorbed *A*, although they have the same value of adsorption density. ΔG_1 and K_{eq} are the change in Gibbs free energy and equilibrium constant of step 1, respectively. ΔG_2 of step 2 is the difference in Gibbs free energy between the reaction products of the real irreversible process [1] and the ideal reversible process (step 1) . K_{me} is the equilibrium constant of step 2.

Thus,

$$\Delta G_{real} = \Delta G_1 + \Delta G_2 \tag{3}$$

since

$$\Delta G = -RT \ln K$$

Thus,

$$K_{real} = K_{eq} \times K_{me} \tag{4}$$

In step2

$$\Delta G_2 = \left(G_{H_2O} + G_A^{solid}\right)_{real} - \left(G_{H_2O} + G_A^{solid}\right)_{ideal} \tag{5}$$

assuming

$$\left(G_{H_2O}\right)_{real} = \left(G_{H_2O}\right)_{ideal}$$

$$\Delta G_2 = \left(G_A^{solid}\right)_{real} - \left(G_A^{solid}\right)_{ideal} \geq 0 \tag{6}$$

where ''='' represents a reversible process and ''>'' corresponds to an irreversible process. Equation [6] indicates that if the process is not thermodynamically reversible, then for the same amount of adsorbed A, the real state of , which is of metastable equilibrium in nature, will have a higher Gibbs free energy $\left(G_A^{solid}\right)_{real}$ than the ideal equilibrium state $\left(G_A^{solid}\right)_{ideal}$. Step 2 is therefore not a thermodynamically spontaneous process.

Since $K_{\text{me}} = e^{-\Delta G_2/RT}$ and $\Delta G_2 \geq 0$,

$$0 < K_{me} \leq 1 \quad (< \text{for irreversible process, = for reversible process}). \tag{7}$$

We call K_{me} the metastable-equilibrium coefficient. It measures the deviation of a metastable-equilibrium state from the ideal equilibrium state. Combining [4] and [7], we get the *MEA inequality*:

$$K_{\text{real}} \leq K_{\text{eq}} \quad (< \text{for irreversible process, = for reversible process}). \tag{8}$$

K_{eq} is the ideal equilibrium constant for an ideal reversible process which has a unique value under constant temperature, pressure, and composition of the solution. K_{real} is the experimentally measured equilibrium constant for a real adsorption process and is not necessarily constant under fixed temperature, pressure, and composition of solution, but decreases as K_{me} decreases.

MEA inequality indicates that equilibrium constants or adsorption isotherms are fundamentally affected by the kinetic factor of thermodynamic irreversibility (including both mass and energetic irreversibility for a forward-backward reaction), because when the surface reaction is processed through different irreversible kinetic pathways it may reach to different MEA states under the same thermodynamic conditions. By using the MEA inequality to reformulate the existing equilibrium adsorption theories, it is possible to modify some of the existing isotherm equations into metastable-equilibrium equations.

2.1 Langmuir-type metastable equilibrium adsorption isotherm

The equilibrium constant for the adsorption process [1] is

$$K_{\text{real}} = \frac{\left(a_A\right)_s \times \left(a_{H_2O}\right)_l}{\left(a_{H_2O}\right)_s \times \left(a_A\right)_l} = \frac{\left(f_A\right)_s \times \left(x_A\right)_s \times \left(a_{H_2O}\right)_l}{\left(f_{H_2O}\right)_s \times \left(x_{H_2O}\right)_s \times \left(a_A\right)_l} \tag{9}$$

where a_{i} stands for the activity of a given component in [1], the subscripts s and l refer to surface and bulk values, respectively, $(f_i)_{\text{s}}$ is the surface activity coefficient, and $(x_i)_{\text{s}}$ is the mole fraction surface concentration.

In dilute solution, the surface activity coefficient in the solid may be set equal to unity (1), so that

$$K_{\text{real}} = \frac{\left(x_A\right)_s \times \left(a_{H_2O}\right)_l}{\left(x_{H_2O}\right)_s \times \left(a_A\right)_l} \tag{10}$$

According to Eq. [4], we have

$$K_{\mathrm{eq}} \times K_{me} = \frac{(x_A)_s \times (a_{H_2O})_l}{(x_{H_2O})_s \times (a_A)_l} \tag{11}$$

By multiplying both $(x_A)_s$ and $(x_{H_2O})_s$ by the total surface area A_T, and assuming that the molecular size of solute and solvent are similar, we have $\theta_A = (x_A)_s \times A_T$, and $\theta_{H_2O} = (x_{H_2O})_s \times A_T$, where θ_i is the fraction of the surface occupied by component *i*. Because $\theta_A + \theta_{H_2O} = 1$, [11] becomes

$$\theta_A = \frac{K_{eq} \times K_{me} \times (a_A)_l}{(a_{H_2O})_l} \Big/ 1 + \frac{K_{eq} \times K_{me} \times (a_A)_l}{(a_{H_2O})_l} \tag{12}$$

Since the activity of solvent $(a_{H_2O})_l$ can be considered constant, $K_{\mathrm{eq}}/(a_{H_2O})_l$ may be defined as a constant *b*,

$$\theta_A = \frac{b \times K_{me} \times (a_A)_l}{1 + b \times K_{me} \times (a_A)_l} \tag{13}$$

Practically, the adsorption amount is often expressed in terms of the adsorption density Γ; thus,

$$\theta = \frac{\Gamma}{\Gamma_{\max}} \tag{14}$$

where $\Gamma_{\max}$ is the characteristic saturation adsorption capacity for a given reaction, which is the maximum value of the equilibrium Γ as the equilibrium concentration of the solute increases. In dilute solution, activity $(a_A)_l$ is approximately equal to concentration C_A, so [13] becomes

$$\Gamma = \frac{b' \times K_{me} \times C_{eq}}{1 + b' \times K_{me} \times C_{eq}} \tag{15}$$

where $b' = b \times \Gamma_{\max}$; b and b' are constant under fixed temperature and pressure, and are truly independent of the kinetics of the process.

Equations [13] and [15] are called *Langmuir-type metastable-equilibrium isotherm equations,* since when K_{me} =1, i.e., under the ideal equilibrium condition, they are reduced to the conventional Langmuir equation. Only under this ideal condition (K_{me} = 1) can the isotherm be independent of the kinetic process. Generally, the equilibrium relationship between Γ and C_{eq} would be influenced by the metastability of the adsorption state.

2.2 Freundlich-type metastable-equilibrium adsorption isotherm

By assuming an exponential distribution of adsorption energy, and assuming that for each energy level the adsorbate coverage θ follows the Langmuir-type metastable-equilibrium isotherm [13] , a Freundlich-type metastable isotherm equation can be obtained,[12]

$$\Gamma = \alpha \times K_{me} \times C_{eq}^{\beta} \tag{16}$$

where α is a constant under isothermal conditions. Under ideal equilibrium conditions (K_{me} = 1) , [16] is reduced to the conventional Freundlich equation. Equation [16] indicates that the adsorption isotherm is shifted to the lower Γ as K_{me} decreases.

2.3 Particle concentration (C_p) effect isotherm equations

According to reaction rate theory, adsorption speed should increase as particle concentration (i.e., reactant concentration) increases.[15, 16] Since the reversibility for a physical adsorption process on a plain solid surface generally declines as the speed of the process increases, the adsorption reversibility could decline as the particle concentration increases. Here, we assume that changes in C_p can affect the metastable-equilibrium adsorption state,

$$K_{me} = \gamma \times C_p^{-n} \tag{17}$$

where γ is a constant and n is an empirical parameter, $n \geq 0$.

Substituting [17] into [15] , we obtain a semi-empirical Langmuir-type C_p effect isotherm equation

$$\Gamma = \frac{k' \times C_p^{-n} \times C_{eq}}{1 + k \times C_p^{-n} \times C_{eq}} \tag{18}$$

where $k' = b' \times \gamma$ and $k = b \times \gamma$. For a given adsorption reaction, k' and k are equilibrium adsorption constants which are independent of the C_{eq} and C_p conditions.

Substituting [17] into [16] , we obtain a Freundlich-type C_p effect isotherm equation,

$$\Gamma = k_{sp} \times C_p^{-n} \times C_{eq}^{\beta} \tag{19}$$

where $k_{sp} = \alpha \times \gamma$. For a given adsorption reaction, k_{sp} is an equilibrium adsorption constant which is independent of the C_{eq} and C_p conditions.

The C_p effect isotherm equations [18] and [19] predict that, by affecting the metastable-equilibrium adsorption state (or the adsorption reversibility), particle concentration can fundamentally influence the equilibrium constants or adsorption isotherms.

3. Macroscopic thermodynamic evidences of metastable-equilibrium adsorption

After Screening study of many adsorption systems, we found that there are obvious C_p effect in many irreversible adsorption systems (e.g., Zn-goethite, Zn-manganite, Zn-anatase, As(V)-anatase), and no C_p effect in reversible adsorption systems (e.g., Cd-goethite and Zn-δ-MnO_2). Taking the adsorption of Zn and Cd on goethite as a typical example, the detailed interpretation of the existence and disappearance of the C_p effect using the metastable-equilibrium adsorption (MEA) theory are presented below.[11, 17]

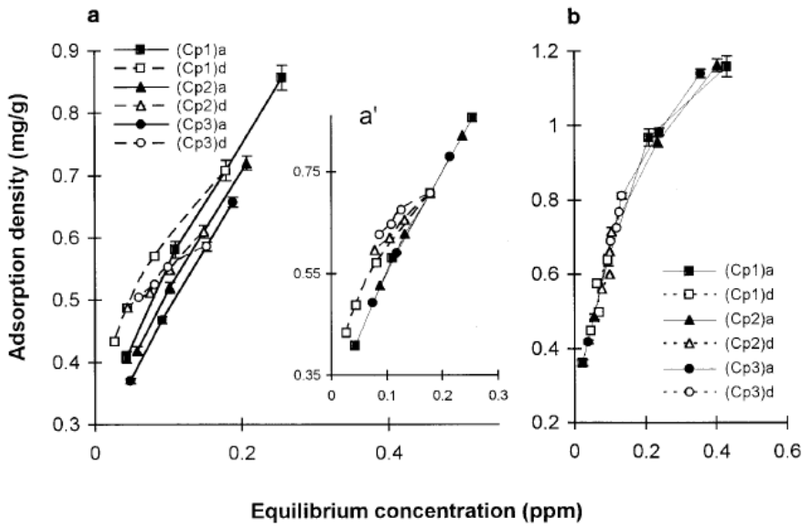

Fig. 1. Adsorption (solid lines, closed symbols) and desorption (dotted lines, open symbols) isotherms under different C_p conditions in Zn–goethite (a) and Cd–goethite (b) systems. (a) C_p1=0.38 g/L, C_p2=1.53 g/L, C_p3=2.3 g/L, pH=6.4, equilibration time for adsorption and desorption are 12 days and 10 days, respectively. a', a comparison of the sizes of hysteresis in Figure 1a, when the first points of the desorption isotherms are translationally moved to the same point. (b) pH=7.1, equilibration time for adsorption and desorption are 20 days and 14 days, respectively.

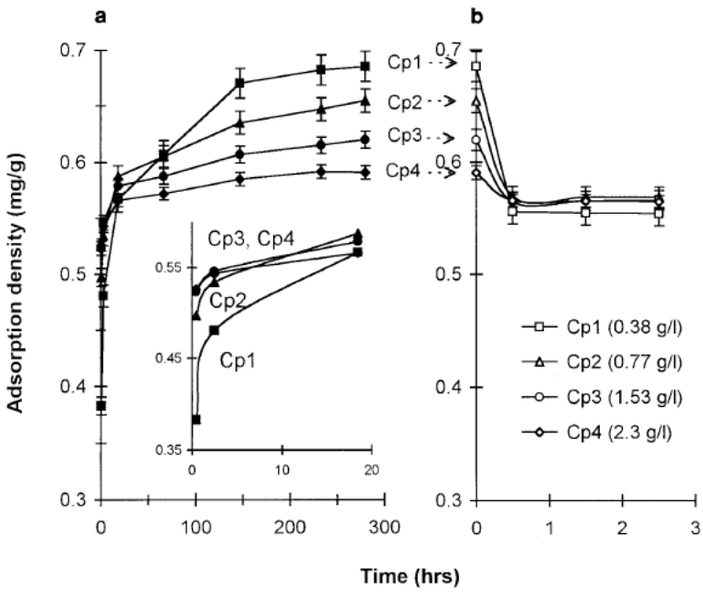

Fig. 2. Adsorption (a) and desorption (b) kinetic curves under different C_p conditions in Zn–goethite system. pH=6.4. The inset chart in (a) shows the initial stage of the adsorption. The final Zn concentrations of the four experiments in (a) are $(C_{eq})_{Cp1}$=0.18 ppm, $(C_{eq})_{Cp2}$=0.17 ppm, $(C_{eq})_{Cp3}$=0.16 ppm, $(C_{eq})_{Cp4}$=0.15 ppm. In order to examine the desorption rate effectively, only the initial stage of desorption is presented in (b).

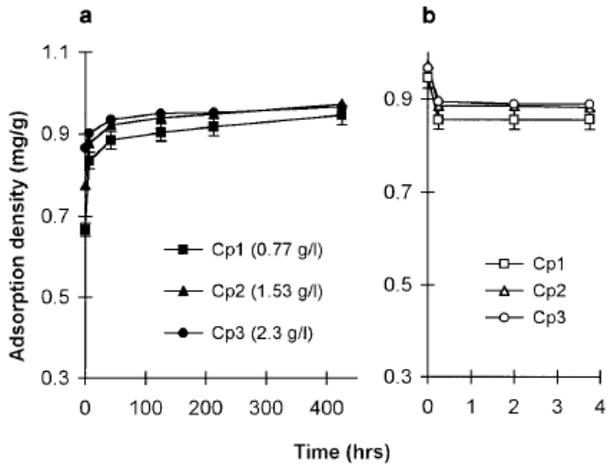

Fig. 3. Adsorption (a) and desorption (b) kinetic curves under different C_p conditions in Cd–goethite system. pH=7.1. The final Cd concentrations of the three experiments in (a) are $(C_{eq})_{Cp1}$=0.235 ppm, $(C_{eq})_{Cp2}$=0.211 ppm, $(C_{eq})_{Cp3}$=0.210 ppm.

In a controlled simple aqueous system containing Zn–goethite, where a clear C_p effect is observed, an increase in particle concentration causes a simultaneous decrease in adsorption reversibility and in the adsorption isotherm (Figure 1a). At the same time, Zn adsorbed under a lower C_p condition desorbs faster (indicating more adsorption reversibility) than that under a higher C_p condition (Figure 2). In another controlled simple aqueous system of Cd–goethite, where no C_p effect is observed, changes in C_p does not cause discernible changes in adsorption hysteresis and in the adsorption isotherm (Figure 1b). Little difference in desorption rate is observed for the Cd adsorbed under different C_p conditions (Figure 3). Both the C_p effect and the non-C_p effect results can be qualitatively explained and quantitatively described by the MEA theory.

In the Freundlich-type C_p effect isotherm equation [19], we called k_{sp} the specific adsorption constant and n the C_p effect index. k_{sp} is a measure of adsorption capacity and n is a measure of the degree of the C_p effect. Like b, k_{sp} and n can be calculated from adsorption isotherm data. The method is described below.

Take the logarithm of both sides of Eq. [19] ,

$$\log\Gamma = \log k_{sp} - n\log C_p + \beta\log C_{eq} \tag{20}$$

For a given adsorption isotherm (e.g., isotherm a, b, or c in Figure 4) , C_p is a constant, and Eq. [20] becomes:

$$\log\Gamma = A + \beta\log C_{eq} \tag{21}$$

where $A = \log k_{sp} - n\log C_p$. It can be seen from [21] that, if the relationship between Γ and C_{eq} under a specified C_p condition can be described by Eq. [19], then the plot of $\log\Gamma$ vs $\log C_{eq}$ should be a straight line. From the slope of the straight line, β can be obtained. Under a given C_{eq} (e.g., data for ' Γ_1 , C_p1,' ' Γ_2 , C_p2,' ' Γ_3 , C_p3' in Figure 4), Eq. [20] becomes

$$\log\Gamma = B - n\log C_p \tag{22}$$

where $B = \log k_{sp} + \beta \log C_{eq}$. Under this condition, if the plot of $\log\Gamma$ vs $\log C_p$ is a straight line, then the influence of C_p on the isotherm can be described by Eq. [19]. From the slope of the straight line, n is obtained.
From the intercepts of either Eq. [21] or Eq. [22], k_{sp} can be calculated.
Based on the adsorption isotherm data of Figure 1, the plots of $\log\Gamma$ vs $\log C_{eq}$ and the plots of $\log\Gamma$ vs $\log C_p$ for Zn–goethite and Cd–goethite systems are presented in Figure 5 and 6, respectively. Good linear relationships were obtained. For the Zn–goethite system, k_{sp}=1.381, β=0.4136, n=0.0819. For the Cd–goethite system, k_{sp}=1.778, β=0.435, n ≈ 0.

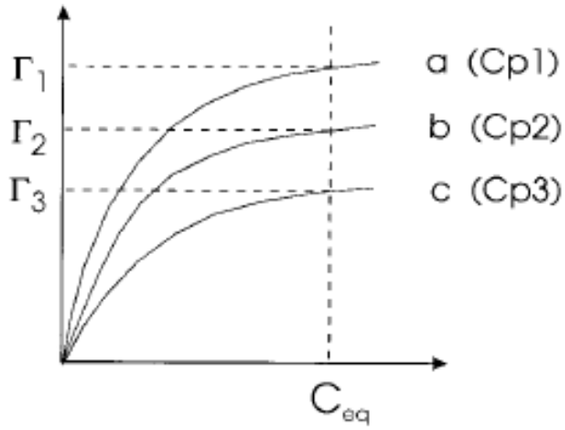

Fig. 4. Data of (Γ , C_{eq}) under constant C_p are used to calculate b. Data of (Γ , C_p) under constant C_{eq} are used to calculate n.

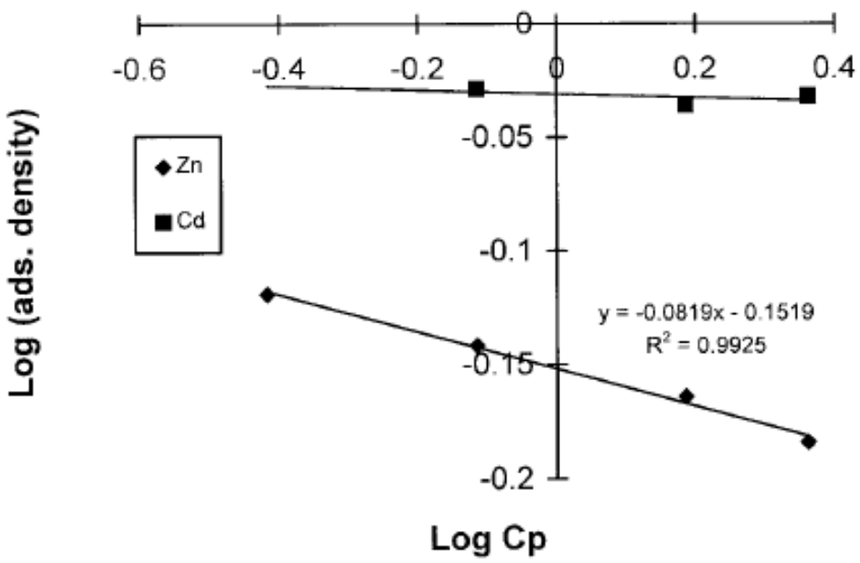

Fig. 5. Plot of $\log C_p$ vs $\log\Gamma$ under the condition of C_{eq}=0.2 ppm for Zn–goethite and Cd–goethite systems, respectively. The different slopes of the two lines indicate that the size of the C_p effect is different in these two systems.

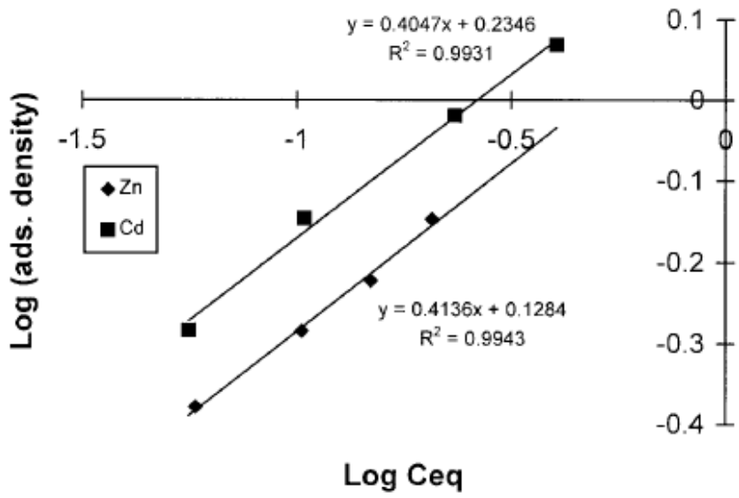

Fig. 6. Plot of $\log C_{eq}$ vs $\log \Gamma$ under the condition of C_p=1.534 g/L for Zn–goethite and Cd–goethite systems, respectively. The similar slope of the two lines indicates that both the adsorption of Zn and Cd on goethite have similar β values.

After the specific adsorption constant (k_{sp}), the C_p effect index (n), and β are calculated, the C_p effect adsorption isotherm equations for Zn–goethite and Cd–goethite systems can be expressed as $\Gamma = 1.381 \times C_p^{-0.0819} \times C_{eq}^{0.4136}$ and $\Gamma = 1.778 \times C_{eq}^{0.435}$, respectively. Figures 7 and 8 show that the calculated isotherms fit the experimental data well.

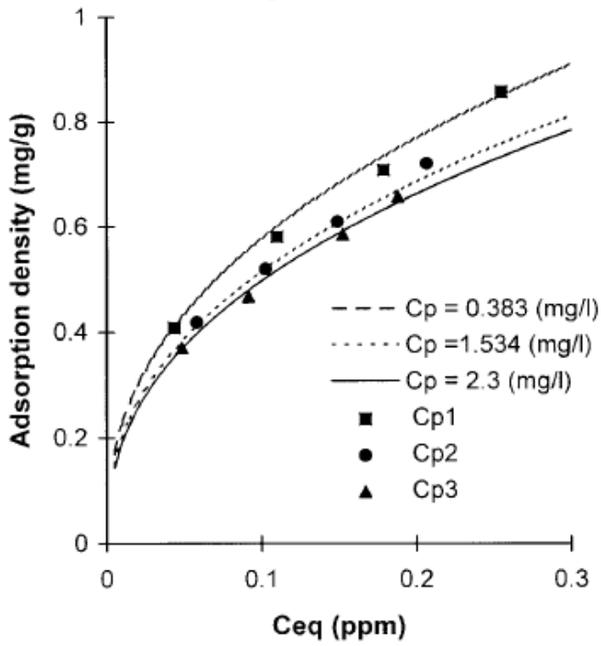

Fig. 7. Comparison between calculated and measured isotherms under different C_p conditions in the Zn–goethite system. Lines are calculated from the C_p effect isotherm equation $\Gamma = 1.381 \times C_p^{-0.0819} \times C_{eq}^{0.4136}$. Points are adsorption data from Figure 1a.

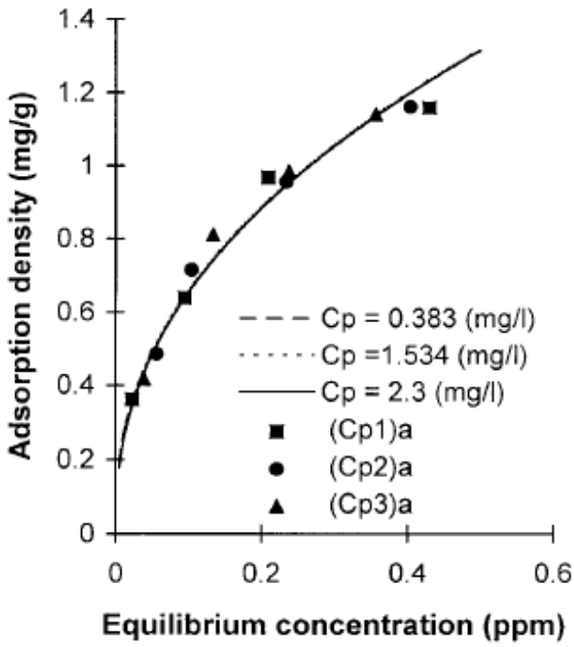

Fig. 8. Comparison between calculated and measured isotherms under different C_p conditions in Cd–goethite system. Lines are calculated from the C_p effect isotherm equation $\Gamma = 1.778 \times C_{eq}^{0.435}$. Points are adsorption data from Figure 1b.

According to MEA theory, for the ideal reversible adsorption reactions, changes in C_p have no influence on the reversibility of MEA states, and it should have no C_p effect in such systems when experimental artifacts are excluded.[11, 18] For partially irreversible adsorption reactions, changes in C_p may significantly affect the irreversibility and the microscopic MEA structures, and a C_p effect should fundamentally exist in irreversible adsorption systems.[11, 17] Therefore, the MEA theory provided a rational explanation for the phenomena of C_p effect and non-C_p effect from the fundamental thermodynamic principle.

4. Microscopic measurement of metastable-equilibrium adsorption state

It should be noted that, when the C_p effect isotherm equations are used in the modeling of practical adsorption processes, they may be totally empirical and does not imply particular physical mechanism. The macroscopic adsorption behavior is fundamentally controlled by the microscopic reaction mechanism of adsorbed molecules on solid surfaces. Therefore, the direct Measurement on the microstructures at solid-water interfaces is crucial to verifying the MEA principle.

Macroscopic thermodynamic results[19, 20] showed that Zn(II) adsorbed on manganite was largely irreversible (adsorption and desorption isotherms corresponding to the forward and backward reactions did not coincide, see Figure 9), but the adsorption of Zn (II) on δ-MnO_2 was highly reversible (there was no apparent hysteresis between the adsorption and desorption isotherms, see Figure 10). This contrast adsorption behavior between the two forms of manganese oxides could be explained from the different microscopic structures

between δ-MnO_2 and manganite, as well as the linkage modes of adsorbed Zn(II) on δ-MnO_2 and manganite.[19]

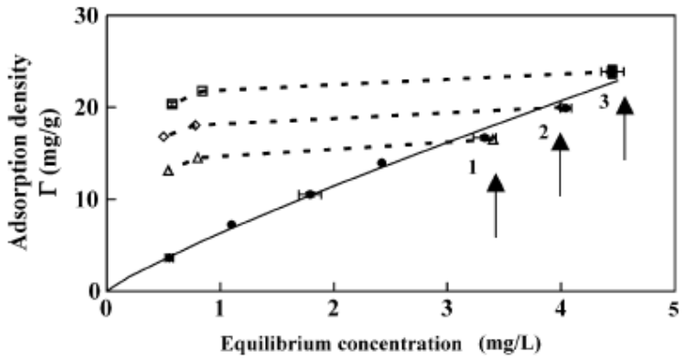

Fig. 9. Adsorption (closed symbols) and desorption (open symbols) isotherms of Zn(II) on manganite. EXAFS samples were indicated by arrows.

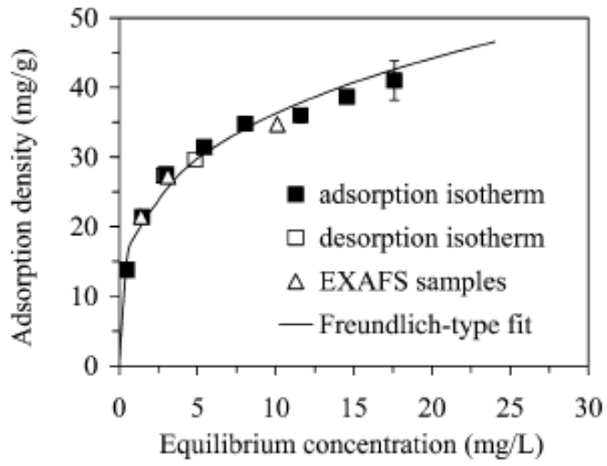

Fig. 10. Adsorption (■) and desorption (□) isotherms of Zn(II) on δ-MnO_2. EXAFS samples were symboled with blank triangles (Δ).

Manganite had a structure with rows of edge-sharing Mn(II)O_6 octahedra linked to adjacent rows through corners. Due to the Jahn–Teller effect of Mn(II) ions and to the presence of both O and OH groups, the MnO_6 octahedra were highly distorted: each Mn is bound to four equatorial oxygen and two axial oxygen atoms.[21, 22] This distortion gave rise to a mild layered structure. Hydrolyzable Zn could be bonded on MnO_6 octahedra of manganite surface via edge and corner-sharing coordination modes.[21, 22] The basic structure of δ-MnO_2 consisted of layers of edge-sharing MnO_6 octahedra alternating with a layer of water molecules. One-sixth of Mn^{4+} positions were empty, which gave a layer charge that was compensated by two Zn atoms located above and below the vacancy.[23, 24] Hydrolyzable Zn could be taken up in the interlayer to form tridentate corner-sharing complexes.[25, 26] These differences in crystallographic structure resulted in different linkage modes for the adsorption of Zn on manganite and δ-MnO_2.

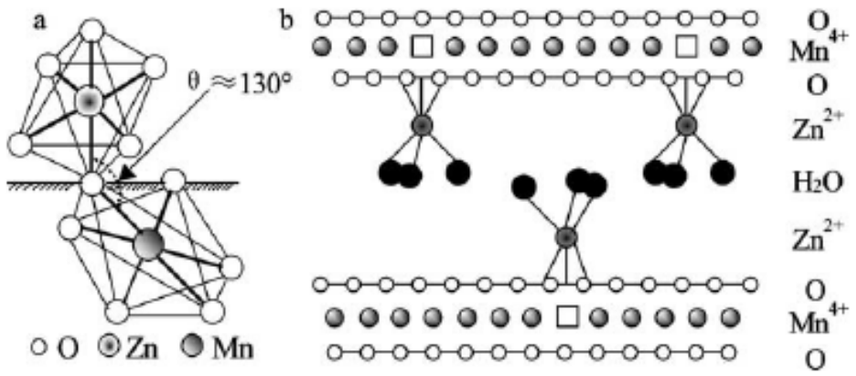

Fig. 11. Corner-sharing linkage (a) and interlayer structures of Zn(II) adsorbed on δ-MnO_2 (b). (a) R_{Zn-O} = 2.07 Å, R_{Mn-O} = 1.92 Å, R_{Zn-Mn} = 3.52 Å. (b) Squares were vacant sites, illustration diagram adapted from Wadsley,[27] Post and Appleman,[28] and Manceau et al..[25]

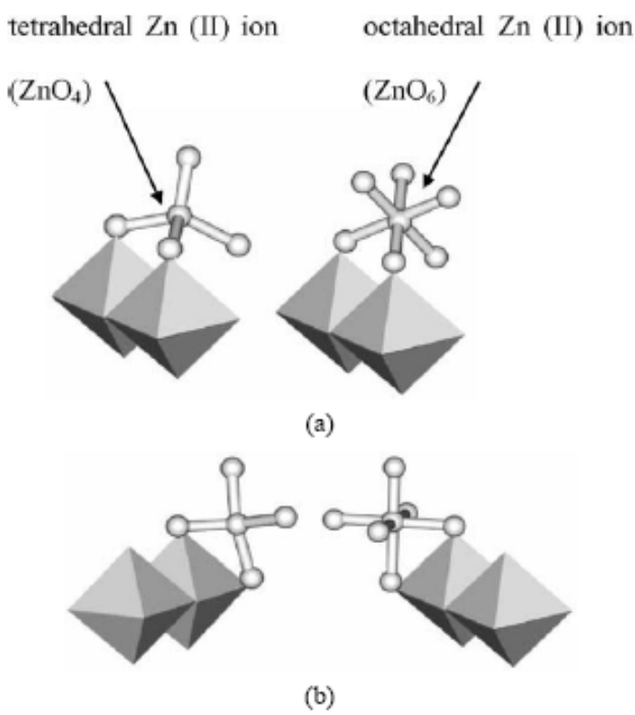

Fig. 12. Two types of linkage between adsorbed Zn(II) (octahedron and tetrahedron) and MnO_6 octahedra on the γ-MnOOH surfaces. (a) Double-corner linkage mode; (b) edge-linkage mode.

Extended X-ray absorption fine structure (EXAFS) analysis showed that Zn(II) was adsorbed onto δ-MnO_2 in a mode of corner-sharing linkage, which corresponded to only one Zn–Mn distance of 3.52 Å (Figure 11). However, there were two linkage modes for adsorbed Zn(II) on manganite surface as inner-sphere complexes, edge-sharing linkage and corner-sharing linkage, which corresponded to two Zn–Mn distances of 3.07 and 3.52 Å (Figure 12). The

edge-sharing linkage was a stronger adsorption mode than that of the corner-sharing linkage, which would make it more difficult for the edge linkage to be desorbed from the solid surfaces than the corner linkage.[20] So adsorption of Zn(II) onto manganite was more irreversible than that on δ-MnO_2. This implied that the adsorption reversibility was influenced by the proportion of different bonding modes between adsorbate and adsorbent in nature.

Due to the contrast adsorption linkage mode, Zn(II) adsorbed on δ-MnO_2 and manganite can be in very different metastable-equilibrium adsorption (MEA) states, which result in the different macroscopic adsorption–desorption behavior. For example, the extents of inconstancy of the equilibrium adsorption constant and the particle concentration effect are very different in the two systems. Adsorption of metals on δ-MnO_2 and manganite may therefore be used as a pair of model systems for comparative studies of metastable-equilibrium adsorption.

5. Temperature dependence of metastable-equilibrium adsorption

Since temperature (*T*) is expected to affect both adsorption thermodynamics and kinetics, the adsorption–desorption behavior may be *T*-dependent. The adsorption irreversibility of Zn(II) on anatase at various temperatures was studied using a combination of macroscopic thermodynamic methods and microscopic spectral measurement.

Adsorption isotherm results[29] showed that, when the temperature increased from 5 to 40 °C, the Zn(II) adsorption capacity increased by 130% (Figure 13). The desorption isotherms significantly deviate from the corresponding adsorption isotherms, indicating that the adsorption of zinc onto anatase was not fully reversible. The thermodynamic index of irreversibility (TII) proposed by Sander et al.[30] was used to quantify the adsorption irreversibility. The TII was defined as the ratio of the observed free energy loss to the maximum possible free energy loss due to adsorption hysteresis, which was given by

$$\mathrm{TII} = \frac{\ln C_{\mathrm{eq}}^{\gamma} - \ln C_{\mathrm{eq}}^{D}}{\ln C_{\mathrm{eq}}^{S} - \ln C_{\mathrm{eq}}^{D}} \tag{23}$$

where C_{eq}^{S} is the solution concentration of the adsorption state S (C_{eq}^{S}, q_{eq}^{S}) from which desorption is initiated; C_{eq}^{D} is the solution concentration of the desorption state D (C_{eq}^{D}, q_{eq}^{D}); C_{eq}^{γ} is the solution concentration of hypothetical reversible desorption state γ (C_{eq}^{γ}, q_{eq}^{γ}). C_{eq}^{S} and C_{eq}^{D} are determined based on the experimental adsorption and desorption isotherms, and are easily obtained from the adsorption branch where the solid-phase concentration is equal to q_{eq}^{D}.

Based on the definition, the TII value lies in the range of 0 to 1, with 1 indicating the maximum irreversibility. The TII value (0.63, 0.34, 0.20) decreased by a factor of >3 when the temperature increased from 5 to 40 °C. This result indicated that the adsorption of Zn(II) on the TiO_2 surfaces became more reversible with increasing temperature.[29]

EXAFS spectra results showed that the hydrated Zn(II) was adsorbed on anatase through edge-sharing linkage mode (strong adsorption) and corner-sharing linkage mode (weak adsorption), which corresponded to two average Zn–Ti atomic distances of 3.25±0.02 and 3.69±0.03 Å, respectively.[29] According to the DFT results (Figure 14),[13] EXAFS measured the

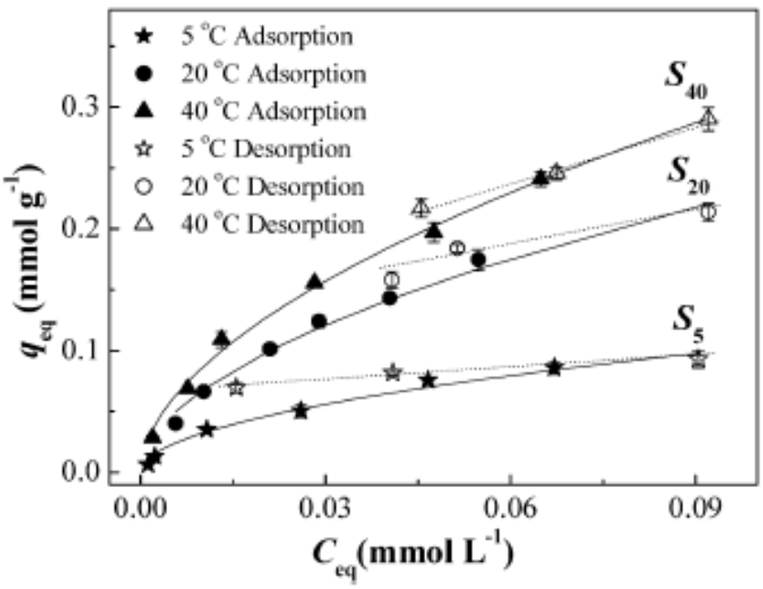

Fig. 13. Adsorption and desorption isotherms of Zn(II) on anatase at various temperatures. Symbols, experimental data; solid lines, model-fitted adsorption isotherms; dashed lines, model-fitted desorption isotherms. S_5, S_{20}, and S_{40} indicate where desorption was initiated and samples selected for subsequent EXAFS analysis. Data given as mean of duplicates and errors refer to the difference between the duplicated samples.

corner-sharing linkage mode at the Zn-Ti distance of 3.69 Å may be a mixture of 4-coordinated bidentate binuclear (BB, 3.48 Å) and 6-coordinated monodentate mononuclear (MM, 4.01 Å) MEA states. DFT calculated energies showed that the MM complex was an energetically unstable MEA state compared with the BB (-8.58 kcal/mol) and BM (edge-sharing bidentate mononuclear, -15.15 kcal/mol) adsorption modes,[13] indicating that the MM linkage mode would be a minor MEA state, compared to the BB and BM MEA state. In the X-ray absorption near-edge structure analysis (XANES), the calculated XANES of BB and BM complexes reproduced all absorption characteristics (absorption edge, post-edge absorption oscillation and shape resonances) from the experimental XANES spectra (Figure 15).[13] Therefore, the overall spectral and computational evidence indicated that the corner-sharing BB and edge-sharing BM complexation mode coexisted in the adsorption of Zn(II) on anatase.

As the temperature increased from 5 to 40 °C, the number of strong adsorption sites (edge linkage) remained relatively constant while the number of the weak adsorption sites (corner linkage) increased by 31%.[29] These results indicate that the net gain in adsorption capacity and the decreased adsorption irreversibility at elevated temperatures were due to the increase in available weak adsorption sites or the decrease in the ratio of edge linkage to corner linkage. Both the macroscopic adsorption/desorption equilibrium data and the molecular level evidence indicated a strong temperature dependence for the metastable-equilibrium adsorption of Zn(II) on anatase.

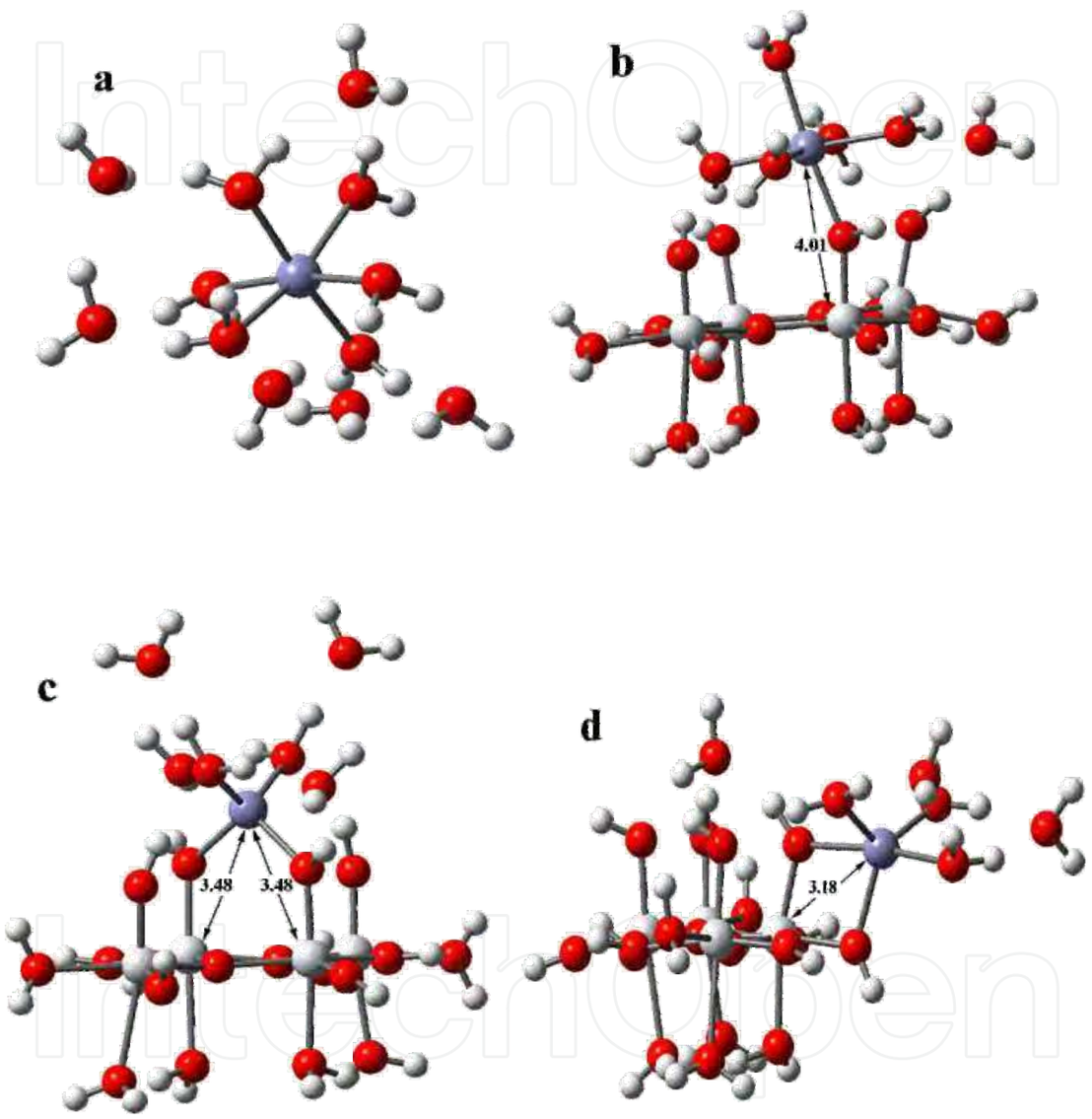

Fig. 14. Calculated Zn(II)–TiO_2 surface complexes using density functional theory: (a) dissolved Zn(II) with six outer-sphere water molecules; (b) monodentate mononuclear (MM); (c) bidentate binuclear (BB); (d) bidentate mononuclear (BM). Purple, red, big gray, small gray circles denote Zn, O, Ti, H atoms, respectively. Distances are shown in angstroms.

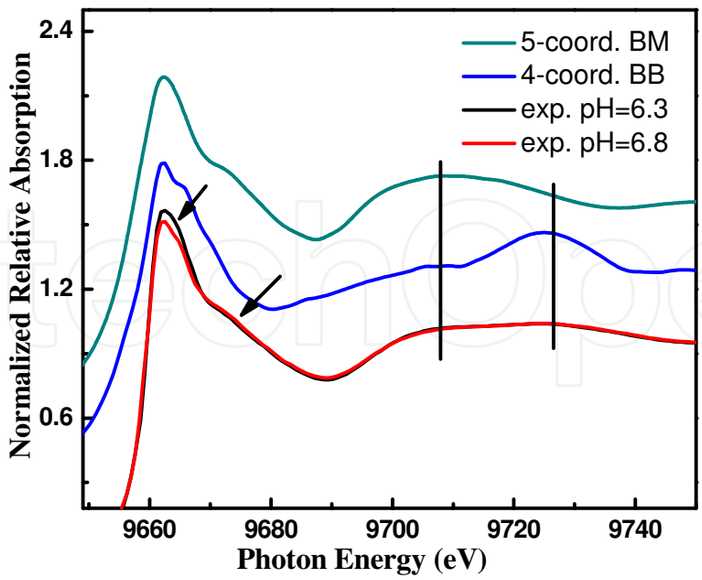

Fig. 15. Calculated XANES spectra of 4-oxygen coordinated BB and 5-oxygen coordinated BM complex and experimental XANES spectra.

6. pH dependence of metastable-equilibrium adsorption

According to MEA theory, both adsorbent/particle concentration (i.e., Cp) and adsorbate concentration could fundamentally affect equilibrium adsorption constants or isotherms when a change in the concentration of reactants (adsorbent or adsorbate) alters the reaction irreversibility or the MEA states of the apparent equilibrium. On the other hand, a general theory should be able to predict and interpret more phenomena. To test new phenomenon predicted by MEA theory can not only cross-confirm the theory itself but also provide new insights/applications in broadly related fields. The influence of adsorbate concentration on adsorption isotherms and equilibrium constants at different pH conditions was therefore studied in As(V)-anatase system using macroscopic thermodynamics and microscopic spectral and computational methods.[14, 31, 32]

The thermodynamic results[14] showed that, when the total mass of arsenate was added to the TiO_2 suspension by multiple batches, the adsorption isotherms declined as the multi-batch increased, and the extent of the decline decreased gradually as pH decreased from 7.0 to 5.5 (Figure 16). This result provided a direct evidence for the influence of adsorption kinetics (1-batch/multi-batch) on adsorption isotherm and equilibrium constant, and indicated that the influence varied with pH.

According to MEA theory, for a given batch adsorption reaction under the same thermodynamic conditions, when the reaction is conducted through different kinetic pathways (1-batch/multi-batch), different MEA states (rather than a unique ideal equilibrium state) could be reached when the reaction reaches an apparent equilibrium (within the experimental time such as days).[14] Equilibrium constants or adsorption isotherms, which are defined by adsorption density, are inevitably affected by the reactant concentration when they alter the final MEA states.[11, 12]

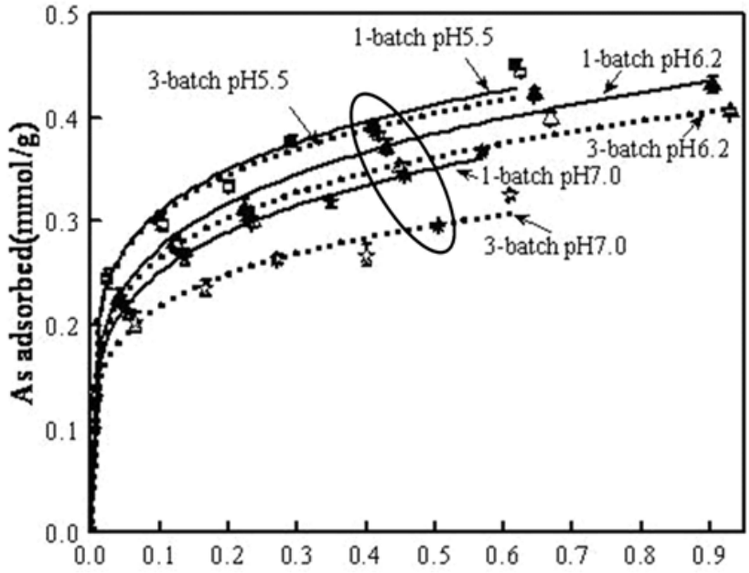

Fig. 16. Adsorption isotherms of As (V) on TiO_2 in 0.01mol/L $NaNO_3$ solution at 25 °C under different pH. TiO_2 particle concentration is 1g/L. 1-batch stands for a series of total arsenate being added to TiO_2 suspension in one time, and 3-batch stands for the total arsenate being added averagely to TiO_2 suspension in 3 times every 4 hours. EXAFS samples were marked by ellipse, in which the initial total As (V) concentration is 0.80 mmol/L.

Sample	As-O			As-Ti						Res.	CN_1/CN_2
				BB			MM				
	CN	R(Å)	σ^2	CN_1	R_1(Å)	σ^2	CN_2	R_2(Å)	σ^2		
1-batch pH5.5	3.9	1.68	0.002	1.9	3.17	0.008	1.1	3.60	0.01	8.6	1.8
3-batch pH5.5	4.0	1.68	0.002	2.2	3.26	0.01	0.9	3.61	0.008	14.2	2.4
1-batch pH6.2	4.0	1.68	0.002	1.8	3.16	0.007	1.0	3.59	0.006	11.0	1.7
3-batch pH6.2	3.9	1.68	0.002	2.1	3.19	0.008	0.8	3.59	0.01	9.0	2.5
1-batch pH7.0	4.1	1.69	0.002	1.8	3.17	0.007	1.1	3.59	0.001	13.2	1.6
3-batch pH7.0	4.1	1.68	0.002	2.2	3.22	0.004	1.0	3.60	0.001	10.9	2.2
As(V)-pH5.5	4.1	1.68	0.004							6.7	
As(V)-pH7.0	4.1	1.69	0.003							5.3	
Calculated values	4.0	1.70		2.0	3.25		1.0	3.52			

Table 1. Summary of As(V) K-edge EXAFS results for 1-batch and 3-batch adsorption samples at pH 5.5, 6.2 and 7.0.

The comparison of EXAFS measured and DFT calculated results indicated that arsenate mainly formed inner-sphere bidentate binuclear (BB) and monodentate mononuclear (MM) surface complexes on TiO_2, where EXAFS measured two As-Ti distances of 3.20±0.05 and 3.60±0.02 Å (Table 1) corresponded to the DFT calculated values of BB (3.25 Å) and MM (3.52 Å) complexes (Figure 17), respectively.[14]

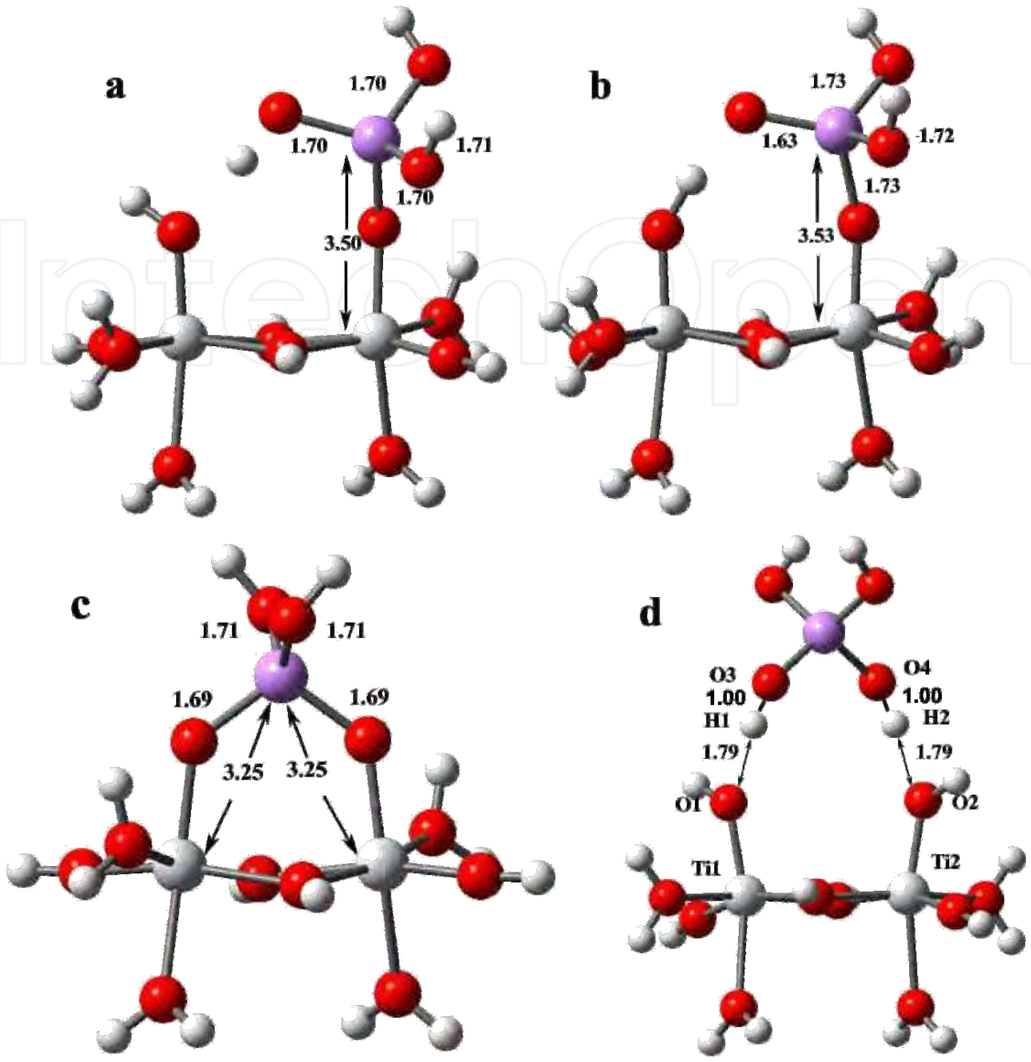

Fig. 17. DFT calculated structure of inner-sphere and H-bond adsorption products of arsenate on TiO_2: (a) monodentate mononuclear arsenate H-bonded to a H_2O surface functional group occupying the adjacent surface site (MM_1); (b) monodentate mononuclear arsenate H-bonded to a -OH surface functional group occupying the adjacent surface site (MM_2); (c) bidentate binuclear (BB) complex; (d) H-bonded complex. Red, big gray, small gray, purple circles denote O, Ti, H, As atoms, respectively. Distances are shown in angstroms.

The EXAFS coordination number of CN_1 and CN_2 represented statistically the average number of nearest Ti atoms around the As atom corresponding to a specific interatomic distance. We used the coordination number ratio of CN_1/CN_2 to describe the relative proportion of BB mode to MM mode in adsorption samples. The CN_1/CN_2 was 1.6 and 2.2 for 1-batch and 3-batch adsorption samples at pH 7.0, respectively (Table 1),[14] indicating that 3-batch adsorption samples contained more BB adsorbed arsenate than that of 1-batch adsorption samples. This result was cross-confirmed by measuring the spectral shift of X-ray absorption near edge structure (XANES) and Fourier transform infrared spectroscopy (FTIR).

DFT calculation showed that the theoretical XANES transition energy of BB complex was 0.62eV higher than that of MM complex. Therefore, the blue-shift of As (V) K-absorption edge observed from 1-batch to 3-batch adsorption samples suggested a structural evolution from MM to BB adsorption as the multi-batch increased (Figure 18).[31]

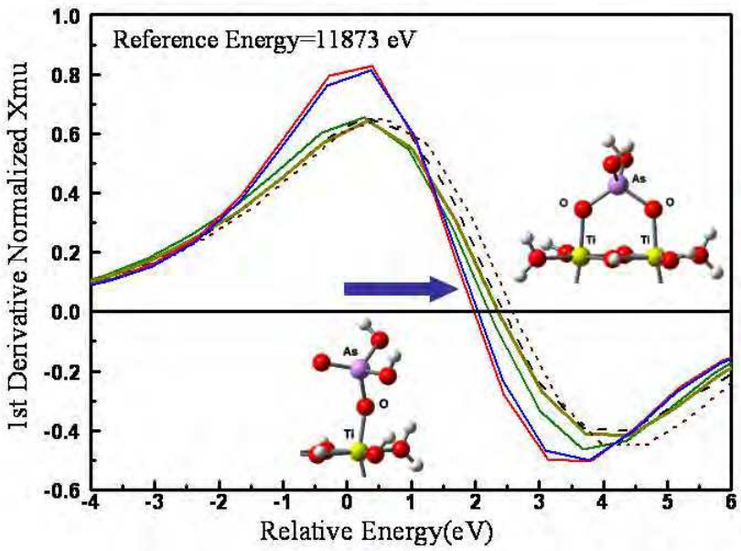

Fig. 18. The first derivative K-edge XANES spectra of As (V) adsorption on anatase.

The DFT calculated frequency analysis showed that the As-OTi asymmetric stretching vibration (υ_{as}) of MM and BB complexes located at 855 and 835 cm-1, respectively. On the basis of this theoretical analysis, the FTIR measured red-shift of As-OTi υ_{as} vibration from 1-batch sample (849 cm-1) to 3-batch sample (835 cm^{-1}) suggested that the ratio of BB/MM in 3-batch sample was higher than that in 1-batch sample (Figure 19).[32]

The good agreement of EXAFS results of CN_1/CN_2 with XANES and FTIR analysis also validated the reliability of the CN ratio used as an index to approximate the proportion change of surface complexation modes. BB complex occupies two active sites on adsorbent surface whereas MM occupies only one. For monolayer chemiadsorption, a unit surface area of a given adsorbent can contain more arsenate molecules adsorbed in MM mode than that in BB mode. Therefore, the increase of the proportion of BB complex from 1-batch to 3-batch addition mode was shown as the decrease of adsorption density in 3-batch isotherm (Figure 16).

Table 1 showed that the relative proportion of BB and MM complex was rarely affected by pH change from 5.5 to 7.0, indicating that the pH dependence for the influence of adsorption kinetics (1-batch/multi-batch) on adsorption isotherm was not due to inner-sphere chemiadsorption.[14] The influence of pH on adsorption was simulated by DFT theory through changing the number of H^+ in model clusters. Calculation of adsorption energy showed that the thermodynamic favorability of inner-sphere and outer-sphere adsorption was directly related to pH (Table 2).[14] As pH decreased, the thermodynamic favorability of inner-sphere and outer-sphere arsenate adsorption on Ti-(hydr)oxides increased. This DFT result explained why the adsorption densities of arsenate (Figure 16) and equilibrium adsorption constant (Table 2) increased with the decrease of pH.

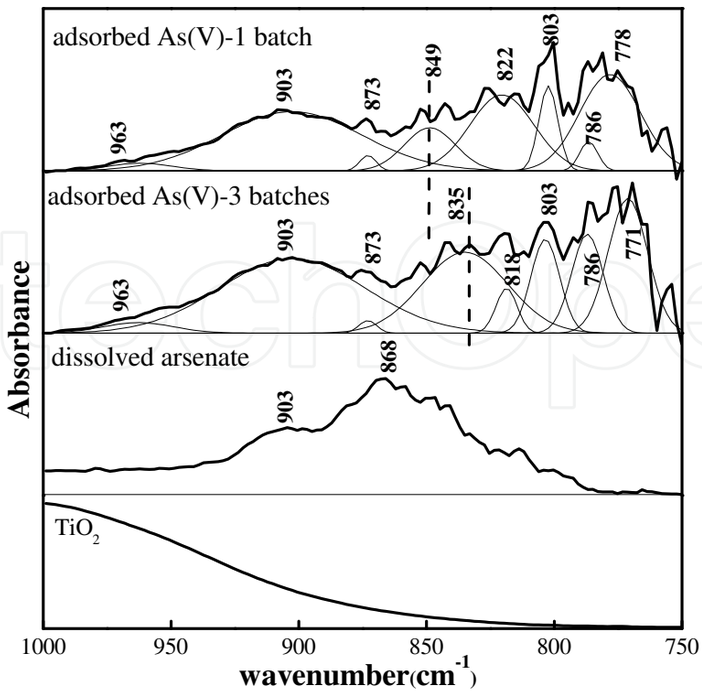

Fig. 19. ATR-FTIR spectra of adsorbed As(V) of 1-batch and 3-batch adsorption samples, dissolved arsenate, and TiO_2 at pH 7.0.

Theoretical equilibrium adsorption constant (K) of calculated surface complexes (BB, MM and H-bonded complexes in this adsorption system) that constructed real equilibrium adsorption constant were significantly different in the order of magnitude under the same thermodynamic conditions (Table 2). The theoretical K were in the order of BB (6.80×10^{42}) >MM (3.13×10^{39}) >H-bonded complex (3.91×10^{35}) under low pH condition, and in the order of MM (1.54×10^{-5}) > BB (8.72×10^{-38}) >H-bonded complex (5.01×10^{-45}) under high pH condition. Therefore, even under the same thermodynamic conditions, the real equilibrium adsorption constant would vary with the change of the proportion of different surface complexes in real equilibrium adsorption.

DFT results (Table 2) showed that H-bond adsorption became thermodynamically favorable (-203.1 kJ/mol) as pH decreased. H-boned adsorption is an outer-sphere electrostatic attraction essentially (see Figure 17d), so it was hardly influenced by reactant concentration (multi-batch addition mode).[14] Therefore, as the proportion of outer-sphere adsorption complex increased under low pH condition, the influence of adsorption kinetics (1-batch/multi-batch) on adsorption isotherm would weaken (Figure 16).

Both the macroscopic adsorption data and the microscopic spectral and computational results indicated that the real equilibrium adsorption state of As(V) on anatase surfaces is generally a mixture of various outer-sphere and inner-sphere metastable-equilibrium states. The coexistence and interaction of outer-sphere and inner-sphere adsorptions caused the extreme complicacy of real adsorption reaction at solid-liquid interface, which was not taken into account in traditional thermodynamic adsorption theories for describing the macroscopic relationship between equilibrium concentrations in solution and on solid surfaces. The reasoning behind the adsorbent and adsorbate concentration effects is that the conventional adsorption thermodynamic methods such as adsorption isotherms, which are

defined by the macroscopic parameter of adsorption density (mol/m^2), can be inevitably ambiguous, because the chemical potential of mixed microscopic MEA states cannot be unambiguously described by the macroscopic parameter of adsorption density. Failure in recognizing this theoretical gap has greatly hindered our understanding on many adsorption related issues especially in applied science and technology fields where the use of surface concentration (mol/m^2) is common or inevitable.

HO/AsO_4	Adsorption reaction equations	ΔG	K
	Bidentate binuclear complexes		
0	$H_2AsO_4^-(H_2O)_{12}+[Ti_2(OH)_4(H_2O)_6]^{4+}\rightarrow [Ti_2(OH)_4(H_2O)_4AsO_2(OH)_2]^{3+}(H_2O)_2+12H_2O$	-244.5	6.80×10^{42}
1	$H_2AsO_4^-(H_2O)_{12}+[Ti_2(OH)_5(H_2O)_5]^{3+}\rightarrow [Ti_2(OH)_4(H_2O)_4AsO_2(OH)_2]^{3+}(H_2O)_2+OH^-(H_2O)_{11}$	13.1	5.15×10^{-3}
2	$H_2AsO_4^-(H_2O)_{12}+[Ti_2(OH)_6(H_2O)_4]^{2+}\rightarrow [Ti_2(OH)_4(H_2O)_4AsO_2(OH)_2]^{3+}(H_2O)_2+2OH^-(H_2O)_{10}$	211.5	8.72×10^{-38}
	Monodentate mononuclear complexes		
0	$H_2AsO_4^-(H_2O)_{12}+[Ti_2(OH)_4(H_2O)_6]^{4+}\rightarrow [Ti_2(OH)_4(H_2O)_5AsO_2(OH)_2]^{3+}H_2O+12H_2O$	-225.4	3.13×10^{39}
1-1	$H_2AsO_4^-(H_2O)_{12}+[Ti_2(OH)_5(H_2O)_5]^{3+}\rightarrow [Ti_2(OH)_4(H_2O)_5AsO_2(OH)_2]^{3+}H_2O+OH^-(H_2O)_{11}$	32.1	2.37×10^{-6}
1-2	$H_2AsO_4^-(H_2O)_{12}+[Ti_2(OH)_5(H_2O)_5]^{3+}\rightarrow [Ti_2(OH)_5(H_2O)_4AsO_2(OH)_2]^{2+}H_2O+12H_2O$	-135.6	5.72×10^{23}
2	$H_2AsO_4^-(H_2O)_{12}+[Ti_2(OH)_6(H_2O)_4]^{2+}\rightarrow [Ti_2(OH)_5(H_2O)_4AsO_2(OH)_2]^{2+}H_2O+OH^-(H_2O)_{11}$	27.5	1.54×10^{-5}
	H-bond complexes		
0	$H_2AsO_4^-(H_2O)_{12}+[Ti_2(OH)_4(H_2O)_6]^{4+}\rightarrow [Ti_2(OH)_4(H_2O)_6AsO_2(OH)_2]^{3+}+12H_2O$	-203.1	3.91×10^{35}
1	$H_2AsO_4^-(H_2O)_{12}+[Ti_2(OH)_5(H_2O)_5]^{3+}\rightarrow [Ti_2(OH)_4(H_2O)_6AsO_2(OH)_2]^{3+}+OH^-(H_2O)_{11}$	54.4	2.96×10^{-10}
2	$H_2AsO_4^-(H_2O)_{12}+[Ti_2(OH)_6(H_2O)_4]^{2+}\rightarrow [Ti_2(OH)_4(H_2O)_6AsO_2(OH)_2]^{3+}+2OH^-(H_2O)_{10}$	252.9	5.01×10^{-45}

Table 2. Calculated ΔG_{ads} (kJ/mol) and equilibrium adsorption constant *K* at 25 °C of arsenate on various protonated Ti-(hydr)oxide surfaces.

Metastable-equilibrium adsorption (MEA) theory pointed out that adsorbate would exist on solid surfaces in different forms (i.e. MEA states) and recognized the influence of adsorption reaction kinetics and reactant concentrations on the final MEA states (various outer-sphere and inner-sphere complexes) that construct real adsorption equilibrium state. Therefore, traditional thermodynamic adsorption theories need to be further developed by taking metastable-equilibrium adsorption into account in order to accurately describe real equilibrium properties of surface adsorption.

7. Acknowledgment

The study was supported by NNSF of China (20073060, 20777090, 20921063) and the Hundred Talent Program of the Chinese Academy of Science. We thank BSRF (Beijing), SSRF (Shanghai), and KEK (Japan) for supplying synchrotron beam time.

8. References

[1] Atkins , P. W.; Paula, J. d., *Physical Chemistry, 8th edition*. Oxford University Press: Oxford, 2006.
[2] Sverjensky, D. A., *Nature* 1993, 364 (6440), 776-780.
[3] O'Connor, D. J.; Connolly, J. P., *Water Res.* 1980, 14 (10), 1517-1523.
[4] Voice, T. C.; Weber, W. J., *Environ. Sci. Technol.* 1985, 19 (9), 789-796.
[5] Honeyman, B. D.; Santschi, P. H., *Environ. Sci. Technol.* 1988, 22 (8), 862-871.
[6] Benoit, G., *Geochim. Cosmochim. Acta* 1995, 59 (13), 2677-2687.
[7] Benoit, G.; Rozan, T. F., *Geochim. Cosmochim. Acta* 1999, 63 (1), 113-127.
[8] Cheng, T.; Barnett, M. O.; Roden, E. E.; Zhuang, J. L., *Environ. Sci. Technol.* 2006, 40, 3243-3247.
[9] McKinley, J. P.; Jenne, E. A., *Environ. Sci. Technol.* 1991, 25 (12), 2082-2087.
[10] Higgo, J. J. W.; Rees, L. V. C., *Environ. Sci. Technol.* 1986, 20 (5), 483-490.
[11] Pan, G.; Liss, P. S., *J. Colloid Interface Sci.* 1998, 201 (1), 77-85.
[12] Pan, G.; Liss, P. S., *J. Colloid Interface Sci.* 1998, 201 (1), 71-76.
[13] He, G. Z.; Pan, G.; Zhang, M. Y.; Waychunas, G. A., *Environ. Sci. Technol.* 2011, 45 (5), 1873-1879.
[14] He, G. Z.; Zhang, M. Y.; Pan, G., *J. Phys. Chem. C* 2009, 113, 21679-21686.
[15] Nyffeler, U. P.; Li, Y. H.; Santschi, P. H., *Geochim. Cosmochim. Acta* 1984, 48 (7), 1513-1522.
[16] Dzombak, D. A.; Morel, F. M. M., *J. Colloid Interface Sci.* 1986, 112 (2), 588-598.
[17] Pan, G.; Liss, P. S.; Krom, M. D., *Colloids Surf., A* 1999, 151 (1-2), 127-133.
[18] Pan, G., *Acta Scientiae Circumstantia* 2003, 23 (2), 156-173(in Chinese).
[19] Li, X. L.; Pan, G.; Qin, Y. W.; Hu, T. D.; Wu, Z. Y.; Xie, Y. N., *J. Colloid Interface Sci.* 2004, 271 (1), 35-40.
[20] Pan, G.; Qin, Y. W.; Li, X. L.; Hu, T. D.; Wu, Z. Y.; Xie, Y. N., *J. Colloid Interface Sci.* 2004, 271 (1), 28-34.
[21] Bochatay, L.; Persson, P., *J. Colloid Interface Sci.* 2000, 229 (2), 593-599.
[22] Bochatay, L.; Persson, P.; Sjoberg, S., *J. Colloid Interface Sci.* 2000, 229 (2), 584-592.
[23] Drits, V. A.; Silvester, E.; Gorshkov, A. I.; Manceau, A., *Am. Mineral.* 1997, 82 (9-10), 946-961.
[24] Post, J. E.; Veblen, D. R., *Am. Mineral.* 1990, 75 (5-6), 477-489.
[25] Manceau, A.; Lanson, B.; Drits, V. A., *Geochim. Cosmochim. Acta* 2002, 66 (15), 2639-2663.
[26] Silvester, E.; Manceau, A.; Drits, V. A., *Am. Mineral.* 1997, 82 (9-10), 962-978.
[27] Wadsley, A. D., *Acta Crystallographica* 1955, 8 (3), 165-172.
[28] Post, J. E.; Appleman, D. E., *Am. Mineral.* 1988, 73 (11-12), 1401-1404.
[29] Li, W.; Pan, G.; Zhang, M. Y.; Zhao, D. Y.; Yang, Y. H.; Chen, H.; He, G. Z., *J. Colloid Interface Sci.* 2008, 319 (2), 385-391.
[30] Sander, M.; Lu, Y.; Pignatello, J. J. *A thermodynamically based method to quantify true sorption hysteresis*; Am Soc Agronom: 2005; pp 1063-1072.

[31] He, G. Z.; Pan, G.; Zhang, M. Y.; Wu, Z. Y., *J. Phys. Chem. C* 2009, 113 (39), 17076-17081.
[32] Zhang, M. Y.; He, G. Z.; Pan, G., *J. Colloid Interface Sci.* 2009, 338 (1), 284-286.

IntechOpen

IntechOpen

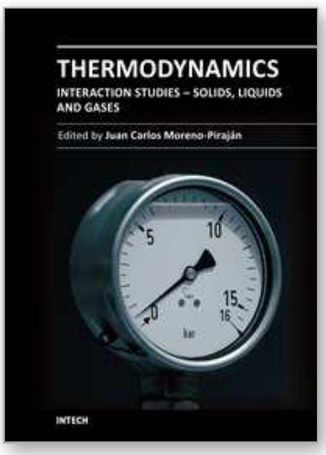

Thermodynamics - Interaction Studies - Solids, Liquids and Gases
Edited by Dr. Juan Carlos Moreno PirajÃ¡n

ISBN 978-953-307-563-1
Hard cover, 918 pages
Publisher InTech
Published online 02, November, 2011
Published in print edition November, 2011

Thermodynamics is one of the most exciting branches of physical chemistry which has greatly contributed to the modern science. Being concentrated on a wide range of applications of thermodynamics, this book gathers a series of contributions by the finest scientists in the world, gathered in an orderly manner. It can be used in post-graduate courses for students and as a reference book, as it is written in a language pleasing to the reader. It can also serve as a reference material for researchers to whom the thermodynamics is one of the area of interest.

How to reference
In order to correctly reference this scholarly work, feel free to copy and paste the following:

Gang Pan, Guangzhi He and Meiyi Zhang (2011). Advances in Interfacial Adsorption Thermodynamics: Metastable-Equilibrium Adsorption (MEA) Theory, Thermodynamics - Interaction Studies - Solids, Liquids and Gases, Dr. Juan Carlos Moreno PirajÃ¡n (Ed.), ISBN: 978-953-307-563-1, InTech, Available from: http://www.intechopen.com/books/thermodynamics-interaction-studies-solids-liquids-and-gases/advances-in-interfacial-adsorption-thermodynamics-metastable-equilibrium-adsorption-mea-theory

INTECH
open science | open minds

InTech Europe
University Campus STeP Ri
Slavka Krautzeka 83/A
51000 Rijeka, Croatia
Phone: +385 (51) 770 447
Fax: +385 (51) 686 166
www.intechopen.com

InTech China
Unit 405, Office Block, Hotel Equatorial Shanghai
No.65, Yan An Road (West), Shanghai, 200040, China
中国上海市延安西路65号上海国际贵都大饭店办公楼405单元
Phone: +86-21-62489820
Fax: +86-21-62489821

© 2011 The Author(s). Licensee IntechOpen. This is an open access article distributed under the terms of the Creative Commons Attribution 3.0 License, which permits unrestricted use, distribution, and reproduction in any medium, provided the original work is properly cited.

IntechOpen

IntechOpen